 http://dx.doi.org/10.7494/mech.2016.35.1.6

JACEK SNAMINA, BOGDAN SAPIŃSKI*

# PHYSICAL MODEL OF VEHICLE ENGINE MOUNT WITH MAGNETORHEOLOGICAL DAMPER

*ABSTRACT*

*A physical model of a vehicle engine mount incorporating a magnetorheological (MR) damper in squeeze mode is investigated and the structural design and operating characteristics of the MR damper are provided. The mathematical model of an engine mount is formulated. Kinematic excitations are assumed to be those emulating road profile--chassis (car body) interactions. Simulations of engine vibration are performed to determine the efficiency of the proposed engine mount. Conclusions are drawn concerning the potential applications of the MR damper in vehicle engine mounts.*

***Keywords:*** *MR damper, engine mount, vibration, model*

*MODEL FIZYCZNY ZAWIESZENIA SILNIKA SAMOCHODOWEGO Z TŁUMIKIEM MAGNETOREOLOGICZNYM*

*W pracy opisano budowę modelu fizycznego zawieszenia silnika samochodowego, w którym zastosowano tłumik z cieczą magnetoreologiczną (MR) działającą w trybie ściskania. Sformułowano model matematyczny zawieszenia. Zakładając wymuszenie kinematyczne modelujące oddziaływanie nierówności drogi na karoserię, przeprowadzono symulacje komputerowe drgań silnika. Oceniono efektywność działania zawieszenia oraz sformułowano wnioski dotyczące możliwości zastosowania tłumika MR w zawieszeniu silnika samochodowego.*

***Słowa kluczowe:*** *tłumik MR, zawieszenie silnika, drgania, model*

## 1. INTRODUCTION

Semi-active systems are now in widespread use, mostly because their energy demand is rather low and they can effectively interact with passive systems. The most distinctive feature of semi-active systems is that their parameters can be varied in the course of their operation, thus enabling the control of damping force in the vibration reduction system. The work performed by a semi-active damper force will always be negative, as the damper will take up energy from the system at each instant.

Vibration reduction systems comprising semi-active components can be provided, *inter alia*, in systems securing a combustion engine to a chassis. A combustion engine has an intricate shape, it is secured to the chassis via fixing elements whose positions and parameters are derived from analyses of the static and dynamic behavior of the entire driving system. Since the causes of engine vibrations cannot be wholly eliminated, the structure of the engine mount is of particular importance, ensuring the correct engine configuration in the engine bay and minimizing the dynamic forces involved in chassis--engine interactions.

Rubber elements are used for securing the engine in its position, as they are small in size and relatively cheap. As new car designs were developed, purpose-built hydraulic mounts were introduced (Dol 1991, Ivers, Singh *et al.* 1992, Flower 1995). The presently developed mount designs utilize controlled semi-active components (Ahmadian, Ahn 1999, Yunhe *et al.* 2001, Southern 2009, Craft *et al.* 2010, Zhang *et al.* 2011, Kim 2012, Sapiński and Krupa 2013, Snamina, Sapiński 2014), as well as active components leading to the more effective reduction of undesired dynamic interactions between the engine and chassis.

The engine mount considered in this paper incorporates a newly-designed squeeze-mode MR damper. The work covers a description of the damper, a mathematical model of the engine-frame system, numerical simulations of the road profiles for the assumed road category, and an analysis of engine vibrations.

## 2. MR DAMPER

A simplified scheme of the damper is shown in Figure 1. The damper housing comprises top and bottom covers and an outer cylinder (1). The top cover and outer cylinder are made of a ferromagnetic material, and the bottom cover is made of a diamagnetic. The piston rod (3) integrated with a non-magnetic ring (9) moves inside the inner cylinder (2), which is made of a diamagnetic material and press-fitted together with the ring (7) in the outer cylinder (1). In the damper's middle section, the inner and outer cylinders are shaped in such a way that MR fluid should flow from underneath the piston to the bottom chamber, acting as a fluid container. This chamber is limited from below by the piston (5) having a small mass and provided with sealing.

* AGH University of Science and Technology, Faculty of Mechanical Engineering and Robotics, Krakow, Poland; snamina@agh.edu.pl, deep@agh.edu.pl

The piston is pressed down by a spring (not indicated in the diagram) placed between the lower piston surface and the damper's bottom cover (8). The spring force gives rise to pressure acting upon the MR fluid in the container. In the damper's middle section, there is a system generating a magnetic field comprising a coil (6) wound on the core (4). Magnetic flux is conditioned in the damper's magnetic circuit, incorporating a coil core, outer cylinder, top cover, and piston, and the volume underneath the piston is filled with MR fluid. Dimensions of the magnetic circuit components are chosen such that the magnetic flux permeating the volume underneath the piston should be sufficient to effectively affect the MR fluid moving radially (as a result of piston movement).

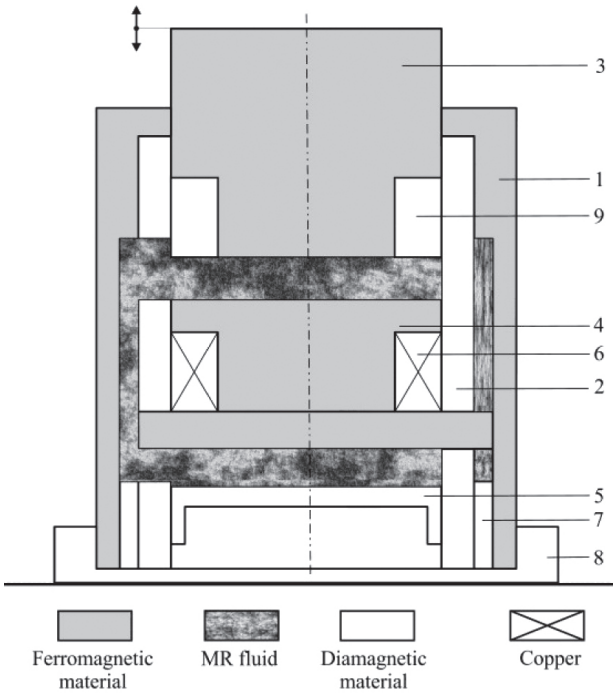


**Fig. 1.** Scheme of MR damper. Explanation in text

During the damper operation, the height of the working gap beneath the piston is a function of time; hence, the magnetic resistance of the circuit will vary, and the magnetic system is non-stationary. A detailed description of the damper's design structure is given elsewhere (Sapiński, Gołdasz 2015).

The damper force (Sapiński 2015) acting upon the vibrating object can be approximated as follows:

$$F_d = \beta_1(\mu, D_p)\frac{1}{h^3}\dot{h} + \beta_2(D_p)\tau_0(I)\frac{1}{h}\operatorname{sgn}(\dot{h}) + \\ + \beta_3(\rho, D_p)\frac{1}{h}\ddot{h} - \beta_4(\rho, D_p)\frac{1}{h^2}\dot{h}^2 \tag{1}$$

where:

$D_p$ – the piston diameter,
$\mu$ – the dynamic viscosity of the MR fluid,
$I$ – the current,
$\rho$ – the density of the MR fluid,
$\tau_0$ – the yield stress of the MR fluid,
$\beta_1 \ldots \beta_4$ – the coefficients determined empirically,
$h$ – the height of the working gap (the displacement between the piston and core surfaces).

The terms expressing particular force components in Equation (1) have their physical interpretation. The first term is associated with fluid viscosity and the second is associated with those parameters of the MR fluid that are related to magnetic induction. The two remaining terms are associated with the inertia of the MR fluid during its flow in the chamber underneath the piston. The second term, associated with the magnetic field induction, appears to be predominant. The damper force is plotted in Figure 2 assuming sine variable movement of the piston with respect to the damper housing (an amplitude of 0.7 mm and frequency of 9 Hz) and the following values of the parameters: $\beta_1 = 7.19 \cdot 10^{-8}$ kg·m$^3$/s; $\beta_2 = 1.02 \cdot 10^{-5}$ m$^3$; $\beta_3 = 1.17 \cdot 10^{-3}$ kg·m; $\beta_4 = 5.87 \cdot 10^{-4}$ kg·m.

In the static equilibrium position, the height of the working gap underneath the piston equals $h_0$. In the context of the damper's design structure, $h_0$ corresponds to the maximal piston displacement in its downward movement with respect to the housing because the piston surface in that position is on the same level as the top surface of the core.

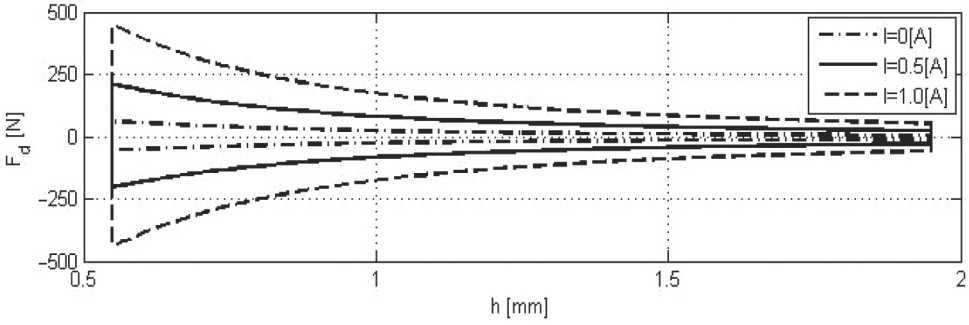


**Fig. 2.** Damper force vs. piston displacement for various current levels; frequency of 9 Hz

## 3. MATHEMATICAL MODEL OF ENGINE-FRAME SYSTEM

Vibrations of the engine and frame associated with the chassis were analyzed by recalling a simplified 2-DOF model. A schematic diagram of the modeled system is shown in Figure 3. The model incorporates an engine as well as a frame that secures the engine in its position in the chassis to which it is directly mounted. The physical model incorporates a prototype MR damper (see MRSQD in Figure 3) as a part of the engine mount, and the applied kinematic excitations emulate interactions caused by road unevenness.

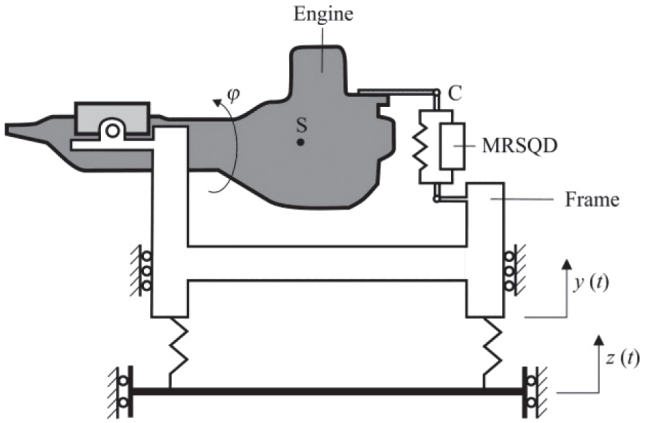


**Fig. 3.** Schematic diagram of investigated system

Equations of the system's vibration are given as follows:

$$\begin{cases} (M+m)\ddot{y} + ml_S\ddot{\varphi} + 4b_p\dot{y} + 4k_p y = 4k_p z(t) \\ J_z\ddot{\varphi} + ml_S\ddot{y} + kl^2\varphi = -F_d l \end{cases} \tag{2}$$

where:

- $M$ – the frame mass,
- $m$ – the engine mass,
- $J_z$ – the inertia moment of the entire engine (incorporating a crankshaft and piston assembly) with respect to the rotation axis of the engine mount,
- $F_d$ – the force of damper-engine block interaction,
- $l$ – the arm of force $F_d$ with respect to the axis of rotation.

Moreover, the damper is assumed to be parallel-connected to a spring with stiffness $k$, $l_S$ is the distance between the engine's center of gravity and rotation axis, angle $\varphi(t)$ expresses the rotation of the engine block, and $y(t)$ is the coordinate of the frame position. Coordinates $\varphi(t)$ and $y(t)$ are determined with respect to the static equilibrium position. The calculation procedure makes use of equivalent viscous damping with factor $b_p$, modeling the damping force in the frame guides.

The term on the right-hand side of the first part of Equation (2) is given in the units of force. Designating $F(t) = 4\,k_p z(t)$, an equivalent scheme of the investigated system (Fig. 4) can be obtained in which kinematic excitations $z(t)$ are replaced by excitations due to force $F(t)$. The direction of force applied to the engine frame passes through the engine's center of gravity. In order to ensure the full model equivalence, the lower spring ends are fixed to the support in equivalent model.

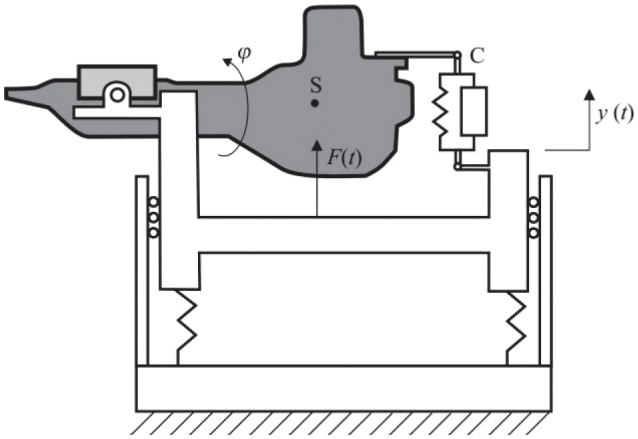


**Fig. 4.** Modified scheme of investigated system

Thus, the equations of the system's vibration can be rewritten as follows:

$$\begin{cases} (M+m)\ddot{y} + ml_S\ddot{\varphi} + 4b_p\dot{y} + 4k_p y = F(t) \\ J_z\ddot{\varphi} + ml_S\ddot{y} + kl^2\varphi = -F_d l \end{cases} \tag{3}$$

The introduction of Equations (3) is associated with the potential ability to use the presented calculations for the construction of the laboratory stand. The analysis of the scheme presented in Figure 4 shows that the laboratory exciter induces the vibrations of the engine block and the engine frame only, while Figure 3 shows that the laboratory exciter also induces the base frame. The load of the laboratory exciter is significantly lower in the case presented in Figure 4.

## 4. SIMULATIONS OF EXCITATIONS

### Due to road unevenness

Road surfaces are not perfect, sporting irregular unevenness whose sizes and frequencies of occurrence are dependent on the quality of the road. Road unevenness occurs regularly, so it has to be handled using a stochastic model. Typically, the power spectral density (PSD) of road unevenness is determined and then used as the criterion for road categorization.

In the case of most vehicles, the resonance frequencies of their subassemblies as well as frequencies posing a hazard to passengers fall within a range of 0.5 to 50 Hz. Assuming the effective velocity range to be 10 to 30 m/s, one determines the wavelengths of road irregularities that vastly contribute to vehicle vibrations. They fall approximately within a range of 0.6 to 20 m, and the corresponding wave numbers are 0.31 to 10.5 rad/m. Road irregularities falling within these estimated ranges are of key importance in the context of vehicle design, passenger safety, ride comfort, and safety of the transported cargo.

Road surface categories are defined in the normative standard, specifying the stochastic parameters of road unevenness for each category of roads. These standard reference values are used in estimate calculations of vibrations of vehicles and their subassemblies.

In simulations, a stationary stochastic process $W(x)$ that is the sum of the sinusoidal processes of the determined amplitudes, determined wave numbers, and random initial phases was used.

$$W(x)=\sum_{j} A_j \sin\left(k_j x+\Phi_j\right) \tag{4}$$

In Equation (4), $A_j$ is the amplitude determined from the assumed PSD, $k_j$ is the wave number calculated in the following way: $k_j = j \cdot k_{\min}$; $j = 1, ..., 60$, where $k_{\min}$ is minimal wave number, and $\Phi_j$ is the random variable with uniform distribution taking values from interval $(-\pi, \pi)$.

The calculation procedure uses the normative power spectral density of road unevenness for A-category roads and involves the simulations of kinematic excitations during a vehicle ride at a velocity of 20 m/s. Figure 5 shows a selected road profile, while Figure 6 plots the kinematic excitations and corresponding PSD values.

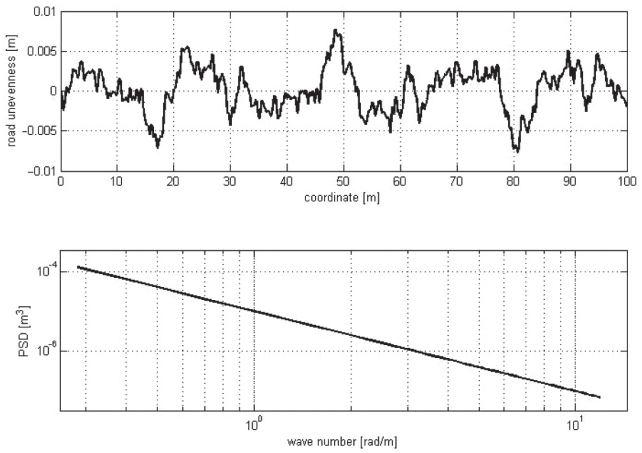


**Fig. 5.** Selected road profile corresponding to normative PSD (A-category road)

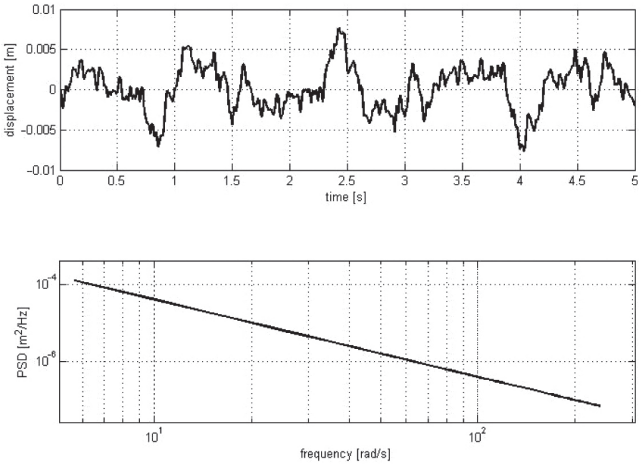


**Fig. 6.** Kinematic excitation and corresponding PSD

With reference to Section 3, kinematic excitation $z(t)$ due to road unevenness is equivalent to force $F(t)$ acting upon the engine frame. Force $F(t)$ has a stochastic nature, and its realizations are associated with the assumed road profile.

## 5. ANALYSIS OF ENGINE VIBRATIONS

Recalling the model of the system and the applied input excitations, calculations were performed to investigate the vibrations of the adopted model – complete with the vibration-reduction system incorporating the MR damper. The first step involved the calculations of vibration modes and frequency followed by calculations of the engine-frame system under the applied excitations emulating the effects of road surface unevenness.

Input data included the parameters obtained from measurements of the individual engine subassemblies and structural design parameters of the MR damper: engine mass and moment of inertia: $m = 75$ kg, $J_z = 20$ kg·m$^2$; mass of the frame $M = 60$ kg; stiffness of the springs in the frame $k_p = 6.6 \cdot 10^3$ N/m; stiffness of the springs in the engine mount $k = 4 \cdot 10^4$ N/m; damping ratio in a factory-made engine mount $b = 641$ Ns/m; equivalent damping ratio in frame guides $b_p = 100$ Ns/m; piston diameter in the MR damper $D_p = 0.064$ m; parameters of MR fluid: density $\rho = 2.45 \cdot 10^3$ kg/m$^3$; dynamic viscosity $\mu = 0.05$ Pa·s.

The calculated natural frequencies with no damping are as follows: $f_1 = 2.1$ Hz; $f_2 = 5.3$ Hz. In the first mode, the coordinate of the relative displacement of the engine with respect to the frame is very small; hence, the influence of the damper is rather minor. In the second mode, these displacements are appreciable.

Simulation results are shown in Figures 7–10. The first plot in each figure presents the relative displacement of the damper piston with respect to the cylinder. The displacement is associated with the engine movement relative to the frame. The second plot shows the frame displacements. The simulation results for a factory-made mount in which the damping is modeled as viscous damping are presented in Figure 7.

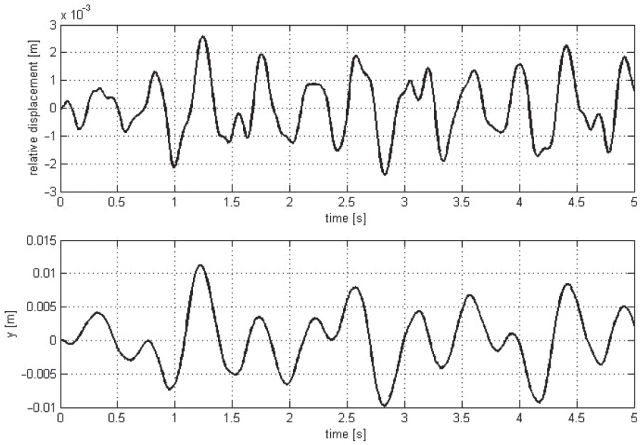


**Fig. 7.** Displacement of viscous damper piston with respect to cylinder and frame displacement (first road profile; the excitation presented in Figure 6)

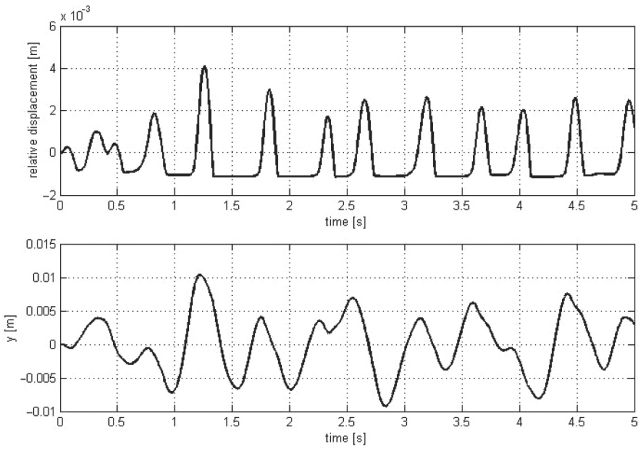


**Fig. 8.** Displacement of MR damper piston with respect to cylinder and frame displacement (first road profile; excitation presented in Figure 6)

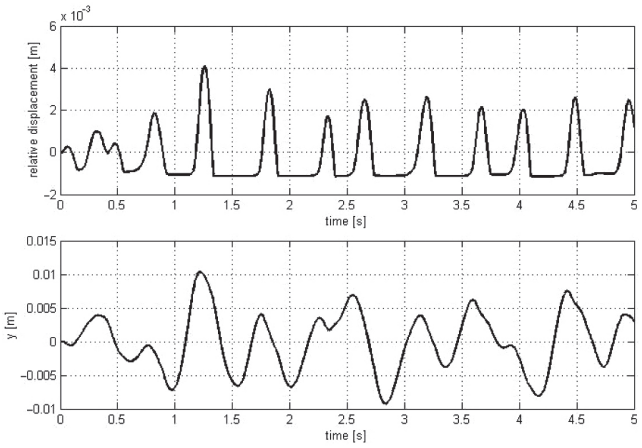


**Fig. 9.** Displacement of MR damper piston with respect to cylinder and frame displacement (second road profile)

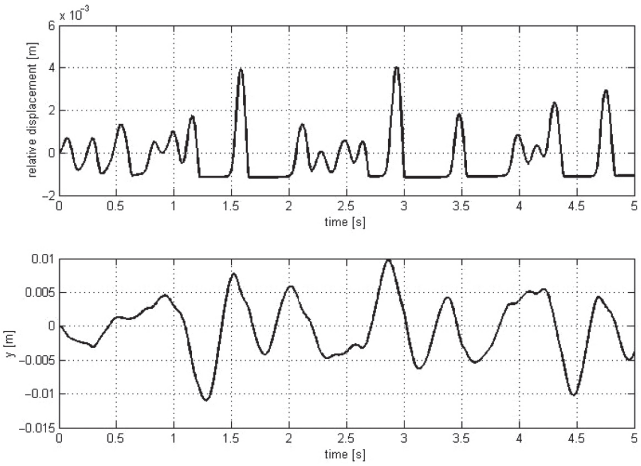


**Fig. 10.** Displacement of MR damper piston with respect to cylinder and frame displacement (third road profile)

Figures 8–10 plot the results of the calculations obtained for a suspension complete with the MR damper. The excitation due to road unevenness shown in Figure 6 was used in the first two cases of the calculations (results presented in Figures 7 and 8). In the latter two cases of the calculations, additionally generated road profiles (for the same PSD) were used.

The calculation results lead us to some conclusions relating to the effectiveness of the MR damper. The effects are apparent, particularly when considering the engine motion with respect to the frame, while in qualitative and quantitative terms, the frame vibrations are on a similar level (even when the MR damper is incorporated). It appears that the nature of relative motion is changed due to the non-symmetry of the damper characteristic. Piston motion when the damper is squeezed involves a much greater force than in extension; hence, the displacement distribution is non-symmetrical. The displacements registered on the squeeze end are considerably smaller than on the extension end. On the squeeze end, there is an instantaneous blocking of the damper; only when the force acting in the opposite direction is sufficiently large can the piston displacements be executed. Actually, the displacements on the extension end can be slightly larger than those registered for a viscous damper. When different road profiles are generated for the same PSD levels, the calculation results will resemble those summarized in Figures 9 and 10. The slight attenuation of the relative vibration cannot be considered as wholly positive. The reduced amplitude of the piston relative motion with respect to the cylinder leads to negative effects as well, as the amount of dispersed energy will be lower. Obviously, the reduction of engine movements with respect to the frame is indicative of the strength of the engine-frame contact.

## 6. CONCLUSIONS

The calculation data summarized in this study was used to estimate the engine vibration associated with the vehicle ride on a road whose surface profile is described by the power spectral density of road unevenness. The results can be useful when designing control algorithms, selecting a system's parameters, and evaluating the performance of the entire vibration reduction system. An obvious disadvantage of the proposed MR damper design is the non-symmetrical characteristic of the damper-engine frame interactions. Variations of force acting when the damper is squeezed can follow different patterns. The lack of symmetry results in the middle position of the engine frame being shifted with respect to the static equilibrium position when vibrations occur. These will not be vibrations around the static equilibrium position. Therefore, the proposed MR damper is effective as long as a control system is used whose algorithm should execute the predetermined vibration reduction method, taking into account the distinctive properties of the MR damper.

**Acknowledgement**

This study has been sponsored under the statutory research grant at AGH-UST, No. 11.11.130.958.

### References

Ahmadian M., Ahn A.K., 1999, *Performance analysis of magneto-rheological mounts*. Journal of Intelligent Material Systems and Structures, 10, 3, 248–256.

Craft M.J., Ahmadian M., Farjud A., Burke W., William C.T., Nagode C., 2010, *Force characterstics of a modular squeeze-mode magneto-rheological element*. Active and Passive Smart Structures and Integrated Systems, Proceedings of the SPIE, 764313; doi: 10.1117/12.848856.

Flower W.C., 1985, *Understanding hydraulic mounts for improved vehicle noise, vibration and ride qualities*. SAE Paper no. 952666.

Ivers D.E., Dol K., 1991, *Semi-active suspension technology: An evolutionary view*. ASME DE-Vol. 40, Advanced Automotive Technologies, Book No. H00719, 1–18.

Kim J.H., 2012, *Damping control device with magnetorheological fluid and engine mount having the same*. United States Patent Application Publication US 2012/0132492A1.

Sapiński B., 2015, *Theoretical analysis of magnetorheological damper characteristics in squeeze mode*. Acta Mechanica et Automatica, 9, 2, 89–92.

Sapiński B., Gołdasz J., 2015, *Development and performance evaluation of an MR squeeze-mode damper*. Smart Materials and Structures, 24, 11, 115007.

Sapiński B., Krupa S., 2013, *Vibration isolator with MR fluid in squeeze mode*. Notification of inventive design No. P.406179.

Singh R., Kim G., Ravindra P.V., 1992, *Linear analysis of automotive hydro-mechanical mount with emphasis on decoupler characteristics*. Journal of Sound and Vibration, 158, 2, 219–243.

Snamina J., Sapiński B., 2014, *Analysis of an automotive vehicle engine mount based on squeeze-mode MR damper*. Technical Transactions – Mechanics, 2-M(13), 53–63.

Southern B.M., 2009, *Design and characterization of tunable magneto-rheological fluid- elastic mounts*. M.S. Thesis, Virginia Polytechnic Institute and State University, Blacksburg.

Yunhe Yu, Nagi G. Naganathan, Rao V. Dukkipati, 2001, *A literature review of automotive vehicle engine mounting systems*. Mechanism and Machine Theory, 36, 123–142.

Zhang X., Zhang H., Ahmadian M., Guo K., 2011, *Study on squeeze-mode magnetorheological engine mount with robust H-infinite control*. SAE Technical Paper 2011-01-0757, doi:10.4271/2011-01-0757.